

Title: Comparison of Diagnostic Performance of Intracoronary Optical Coherence Tomography-based and Angiography-based Fractional Flow Reserve for Evaluation of Coronary Stenosis.

Authors: Jiayue Huang, BSc; Hiroki Emori, M.D; Daixin Ding, BSc; Takashi Kubo, M.D, PhD; Wei Yu, BSc; Peng Huang, BSc; Su Zhang, PhD; Juan Luis Gutiérrez-Chico, M.D, PhD; Takashi Akasaka, M.D, PhD; William Wijns, M.D, PhD; Shengxian Tu, PhD

DOI: 10.4244/EIJ-D-19-01034

Citation: Huang J, Emori H, Ding D, Kubo T, Yu W, Huang P, Zhang S, Gutiérrez-Chico JL, Akasaka T, Wijns W, Tu S. Comparison of Diagnostic Performance of Intracoronary Optical Coherence Tomography-based and Angiography-based Fractional Flow Reserve for Evaluation of Coronary Stenosis. *EuroIntervention* 2020; Jaa-713 2020, doi: 10.4244/EIJ-D-19-01034

Manuscript submission date: 14 November 2019

Revisions received: 15 December 2019, 12 January 2020

Accepted date: 14 January 2020

Online publication date: 21 January 2020

Disclaimer: This is a PDF file of a "Just accepted article". This PDF has been published online early without copy editing/typesetting as a service to the Journal's readership (having early access to this data). Copy editing/typesetting will commence shortly. Unforeseen errors may arise during the proofing process and as such Europa Digital & Publishing exercise their legal rights concerning these potential circumstances.

Comparison of Diagnostic Performance of Intracoronary Optical Coherence Tomography-based and Angiography-based Fractional Flow Reserve for Evaluation of Coronary Stenosis

Jiayue Huang^{1,2}, BSc; Hiroki Emori³, MD; Daixin Ding¹, BSc; Takashi Kubo³, MD, PhD; Wei Yu¹, BSc; Peng Huang¹, BSc; Su Zhang¹, PhD; Juan Luis Gutiérrez-Chico⁴, MD, PhD; Takashi Akasaka³, MD, PhD; William Wijns², MD, PhD; Shengxian Tu¹, PhD

1. Biomedical Instrument Institute, School of Biomedical Engineering, Shanghai Jiao Tong University, Shanghai, China
2. The Lambe Institute for Translational Medicine and Curam, National University of Ireland Galway, Ireland
3. Department of Cardiovascular Medicine, Wakayama Medical University, Wakayama, Japan
4. Department of Interventional Cardiology, Campo de Gibraltar Health Trust, Algeciras, Spain

Disclosures: None

Short running title: Comparison between OFR and QFR

Address for correspondence:

Shengxian Tu, PhD, FACC, FESC

Room123, Med-X Research Institute

Shanghai Jiao Tong University

No. 1954, Hua Shan Road

Shanghai 200030

China

E-mail: sxtu@sjtu.edu.cn

Copyright EuroIntervention

Abstract

Aims

To evaluate the diagnostic performance of OCT-based optical flow ratio (OFR) in unselected patients and compare it with angiography-based quantitative flow ratio (QFR), using wire-based FFR as reference standard.

Methods and Results

All patients with OCT and FFR assessment prior to revascularization were analyzed. OFR and QFR were computed in blinded fashion and compared with FFR, all applying same cut-off value of ≤ 0.80 to define ischemia.

Paired comparison between OFR and QFR was performed in 212 vessels from 181 patients. Average FFR was 0.82 ± 0.10 and 40.1% vessels had $FFR \leq 0.80$. OFR showed significant better correlation and agreement with FFR than QFR ($r=0.87$ versus 0.77 , $p < 0.001$; SD of the difference = 0.05 versus 0.07 , $p < 0.001$). The AUC was 0.97 for OFR, higher than QFR (difference = 0.05 , $p = 0.017$), and much higher than minimal lumen area (difference = 0.15 , $p < 0.001$) and diameter stenosis (difference = 0.17 , $p < 0.001$).

Diagnostic accuracy, sensitivity, specificity, positive predictive value, negative predictive value, positive likelihood ratio, and negative likelihood ratio for OFR to identify $FFR \leq 0.80$ was 92%, 86%, 95%, 92%, 91%, 18.2 and 0.2, respectively.

Diagnostic accuracy of OFR was not significantly different in MI-related vessels (95% versus 90%, $p = 0.456$), nor in vessels with and without previously implanted stents (90%

versus 93%, $p=0.669$).

Conclusions

OFR had an excellent agreement with FFR in consecutive patients with coronary artery disease. OFR was superior than QFR, and much better than conventional morphological parameters in determining physiological significance of coronary stenosis. The diagnostic performance of OFR was not influenced by presence of prior myocardial infarction or implanted stents.

Classifications

Fractional flow reserve, QCA, optical coherence tomography

Condensed Abstract

This study aimed at evaluating the diagnostic performance of OCT-based OFR in unselected patients and compare it with angiography-based QFR. OFR showed significant better correlation and agreement with FFR than QFR ($r=0.87$ versus 0.77 , $p<0.001$; SD of the difference= 0.05 versus 0.07 , $p<0.001$). The AUC was 0.97 for OFR, higher than QFR (difference= 0.05 , $p=0.017$), minimal lumen area (difference= 0.15 , $p<0.001$) and diameter stenosis (difference= 0.17 , $p<0.001$). In conclusion, OFR had an excellent agreement with FFR in consecutive patients with coronary artery disease. OFR was superior than QFR, and much better than conventional morphological parameters in determining physiological significance of coronary stenosis.

Abbreviations and Acronyms

AUC=area under the curve

FFR=fractional flow reserve

ICC=intraclass correlation coefficient

IQR=interquartile range

ISR=in-stent restenosis

MI=myocardial infarction

MLA=minimum lumen area

OFR=optical flow ratio

PCI=percutaneous coronary intervention

QFR=quantitative flow ratio

Copyright EuroIntervention

Introduction

Intracoronary optical coherence tomography (OCT) imaging provides superior image resolution in vivo, allowing detailed assessment of coronary lumen, plaque morphology and stent expansion and apposition¹, while fractional flow reserve (FFR) is the standard of reference to evaluate the functional significance of coronary stenosis². An OCT-based morpho-functional evaluation method based on a single catheter could spare procedure time and cost, whilst being instrumental to overcome the reimbursement constraints that are preventing widespread use of both imaging and physiology for PCI guidance. Recently, a novel and fast OCT-based FFR computational method, hereafter denoted as optical flow ratio (OFR), was developed, allowing assessment of both plaque morphology and coronary physiology using a single OCT image catheter and without the need to induce hyperemia³. However, the diagnostic accuracy of OFR analysis in unselected consecutive patients remains to be performed. In addition, the diagnostic performance of OFR compared with angiography-based quantitative flow ratio (QFR)^{4, 5} has not been evaluated.

Methods

Study design and patient population

This was a retrospective single-center, and observational study, with the primary outcome measure as the diagnostic accuracy of OFR compared with QFR in determining functionally significant stenosis. All patients who underwent both OCT

imaging and FFR assessment between August 1st, 2011 and October 31st, 2018 at Wakayama Medical University Hospital (Wakayama, Japan) were enrolled. Vessels were excluded from OFR analysis if balloon predilatation was performed prior to OCT imaging. OFR was computed in all OCT image pullbacks unless the OCT image quality precluded visualization of the coronary lumen or there was severe image artifact. OFR analysis result was excluded from comparison with FFR if: 1) presence of vessel spasm or injury during OCT imaging; 2) OCT pullback not covering the entire lesion; 3) myocardial bridge in the interrogated vessels; 4) substantial thrombosis identified by OCT; 5) unacceptable quality of the FFR pressure tracings, including calibration, quality of the signals and hyperemic response. Myocardial bridge was defined if the difference of DS% was higher than 20% between systolic and diastolic phases by visual estimation from coronary angiography.

The angiographic images of those patients with paired OFR and FFR were subsequently used for QFR analysis. Exclusion criteria for QFR analysis include: 1) severe overlap at the interrogated vessels; 2) insufficient image quality for TIMI frame count; 3) angiographic views ≤ 25 degrees; 4) severely tortuous vessels; 5) automatic calibration not possible due to missing DICOM parameters.

The study complied with the Declaration of Helsinki for investigation in human beings.

The study protocol was approved by the institutional review board. All patients provided written informed consent.

Coronary angiography, FFR, OCT

Disclaimer : As a public service to our readership, this article -- peer reviewed by the Editors of EuroIntervention - has been published immediately upon acceptance as it was received. The content of this article is the sole responsibility of the authors, and not that of the journal

Details in FFR measurement and acquisition of angiographic images and OCT images are described in Supplementary Data.

OFR and QFR analysis

All angiographic images and OCT images were sent to an academic core laboratory (CardHemo, Med-X Research Institute, Shanghai Jiao Tong University, China) for OFR and QFR analysis, using the OctPlus software (version 1.0) and AngioPlus system (both from Pulse Medical Imaging Technology, Shanghai, China). OFR was analyzed by two experienced analysts (J Huang and D Ding) and were blinded with the QFR and FFR data. QFR was analyzed by another analyst (P. Huang) while being blinded with the OFR and FFR data. The methodologies for OFR and QFR analysis have been described elsewhere^{3, 5}. The difference between these two computational approaches is in the boundary conditions used for the fluid dynamics computation. While QFR reconstructs the lumen geometry from 2 angiographic projections and used modified TIMI frame count to estimate the downstream perfused flow, OFR reconstructs the lumen geometry from OCT and uses a patient-average hyperemic flow velocity in combination with patient-specific reference lumen, i.e., the healthy lumen of the interrogated patient as if there was no stenosis, to estimate the downstream perfused flow. After computation, the OFR and QFR values at the distal position of the analyzed vessel were used to compare with FFR. For interrogated vessels with two OCT pullbacks to cover the entire lesion, the OFR value was computed for each pullback and combined to generate the final OFR value at the most distal position (Supplementary Figure 1).

Diffuse disease was defined if the percentage of OCT image frames without any plaque in the entire pullback was less than 10%. Tandem lesion was defined as two or more stenoses that were separated by angiographically normal segments.

Statistical Analysis

Continuous variables are reported as mean \pm SD if normally distributed or as median (quartiles) if non-normally distributed. Categorical variables are expressed as number (percentage). Correlation was evaluated using Pearson correlation or Spearman correlation as appropriate. Bland-Altman plots and intraclass correlation coefficient (ICC) for the absolute value were used for assessing agreement between different continuous parameters. Comparison of the limit of agreement between OFR and QFR was performed by F-test. Wilcoxon signed-rank test or paired t-test was used for pairwise comparison as appropriate. Diagnostic performance was assessed using the area under the curve (AUC) by receiver-operating characteristic (ROC) analysis. The Youden index was used as the criterion to determine the best cut-off value for OCT-derived MLA and 3D QCA-derived DS% in predicting $FFR \leq 0.80$. Statistical assessments were performed with MedCalc version 14.12 (MedCalc Software, Ostend, Belgium). A 2-sided value of $p < 0.05$ was considered as statistically significant.

Results

Baseline clinical and lesion characteristics

Disclaimer : As a public service to our readership, this article -- peer reviewed by the Editors of EuroIntervention - has been published immediately upon acceptance as it was received. The content of this article is the sole responsibility of the authors, and not that of the journal

Figure 1 shows the study flow chart. A total of 277 consecutive patients undergoing both OCT imaging and pressure-derived FFR measurement were screened. Before the core laboratory analysis, 41 patients were excluded due to the use of balloon predilatation prior to OCT imaging. In the core laboratory 68 vessels were excluded for OFR analysis, mainly due to OCT image pullbacks not covering the entire lesion (59 vessels). Thus, OFR analysis was performed in 230 vessels from 193 patients. The angiographic images of these patients were used for QFR analysis. Eighteen vessels were excluded for QFR analysis, resulting in 212 vessels with paired QFR and OFR results for head-to-head comparison with FFR and for statistical analysis. Baseline demographic and vessel characteristics (Table 1 and 2) show that the interrogated vessels had an average FFR of 0.82 ± 0.10 and median FFR of 0.83 [IQR: 0.76 to 0.91]. FFR ≤ 0.80 was identified in 85 (40.1%) vessels. Bifurcation lesions and tandem lesions were presented in 97 (45.8%) and 47 (22.2%) vessels, respectively. The study population had prior myocardial infarction (MI) in 81 (44.8%) patients with 98 interrogated vessels and prior PCI in 118 (65.2%) patients, with 90 interrogated vessels had previously implanted stents. A total of 77 (36.3%) vessels had FFR value falling in the range between 0.75 and 0.85 and 80 (37.7%) vessels had diffuse disease. Figure 2 shows the histogram distribution of FFR and OFR.

Correlation and agreement

Figure 3 shows a representative case with OFR and QFR computations. Scatter plots and Bland-Altman plots for OFR and QFR in all 212 interrogated vessels (Figure 4)

showed significant better correlation and agreement of OFR with FFR than QFR with FFR ($r=0.87$ versus 0.77 , $p<0.001$; $ICC=0.87$ [95% CI: $0.83-0.90$] versus 0.76 [95% CI: $0.69-0.81$], $p<0.001$). Bland-Altman plot shows better limit of agreement with FFR for OFR than QFR (SD of the difference= 0.05 versus 0.07 , $p<0.001$). The improvement was observed mainly in LAD (Supplementary Table 1).

Diagnostic performance of OFR, QFR, OCT and 3D QCA

The AUC in identifying physiologically significant stenosis was 0.97 [95% CI: $0.93-0.99$] for OFR, which was higher than QFR (difference= 0.05 , $p=0.017$), and much higher than OCT-derived MLA (difference= 0.15 , $p<0.001$) and 3D QCA-based DS% (difference= 0.17 , $p<0.001$) (Figure 5). Using the same cut-off value of ≤ 0.80 to define physiologically significant lesion for OFR, QFR, and FFR, the diagnostic concordance between OFR and FFR was also numerically higher than the concordance between QFR and FFR (92% [95% CI: $88\%-95\%$] versus 87% [95% CI: $83-92$]), though statistically non-significant ($p=0.207$). The improvement was observed in vessels with FFR between 0.80 and 0.90 (Supplementary Figure 2). Sensitivity, specificity, positive predictive value, negative predictive value, positive likelihood ratio and negative likelihood ratio for OFR were 86% , 95% , 92% , 91% , 18.2 and 0.2 , and for QFR were 88% , 87% , 82% , 92% , 7.0 and 0.1 , respectively (Table 3, Figure 6). Diagnostic accuracy of OFR was not influenced by the presence of diffuse disease (92% versus 91% , $p=0.997$). The optimal cut-off value of OCT-derived MLA in predicting $FFR \leq 0.80$ was found at 1.88 mm^2 .

Impact of prior MI on computational FFR

A total of 57 interrogated vessels were related with prior MI. Mean FFR of this group was 0.86 ± 0.10 , compared with 0.81 ± 0.10 in the non-MI-group. The diagnostic accuracy of OFR was not inferior in the MI-group (95% [95% CI: 89%-100%] versus 90% [95% CI: 86%-95%], $p=0.456$). However, the ICC was numerically lower in the MI-group, though statistically non-significant (0.80 [95% CI: $0.69-0.88$] versus 0.88 [95% CI: $0.84-0.91$], $p=0.094$). Similar results were observed for QFR, with a comparable diagnostic accuracy and a numerically lower but statistically non-significant ICC in the MI-group compared with non-MI-group (accuracy: 86% versus 88%, $p=0.911$; ICC: 0.69 versus 0.77 , $p=0.231$). The diagnostic accuracy was better for OFR than QFR in both groups, though statistically non-significant (MI-group: 95% versus 88%, $p=0.204$; non-MI-group: 90% versus 88%, $p=0.586$). Same applied to the ICC with FFR (MI-group: 0.80 versus 0.69 , $p=0.178$; non-MI-group: 0.88 versus 0.77 , $p=0.004$).

Impact of prior PCI on computational FFR

Mean FFR was 0.85 ± 0.10 and 0.80 ± 0.10 in vessels with and without previously implanted stents, respectively. Diagnostic performance of OFR was comparable in vessels with in-stent restenosis (ISR) and in native vessels (AUC= 0.96 versus 0.97 , $p=0.608$). However, there was a trend toward lower diagnostic performance of QFR in vessels with ISR compared with that in native vessels (AUC= 0.88 versus 0.95 ,

p=0.102). The agreement with FFR was better for OFR than QFR in both groups with (ICC=0.84 versus 0.71, p=0.005) and without previously implanted stents (ICC=0.86 versus 0.77, p<0.001).

Discussion

The following points summarize the key findings of the present study: 1) OFR has an excellent agreement with FFR in consecutive patients with a priori high likelihood of PCI. The agreement with FFR was significantly better for OFR than QFR. 2) OFR is superior to QFR, and much better than conventional morphological parameters in diagnosing the physiological significance of coronary stenosis. The diagnostic superiority of OFR over QFR remains regardless the presence of prior PCI or MI. 3) Diagnostic performance of OFR is not significantly different in patients with and without prior MI, nor in native vessels and in vessels with ISR.

This is the first study comparing the diagnostic performance of two novel morpho-functional methods, i.e., OFR and QFR, and two conventional morphological methods, i.e., OCT-derived MLA and 3D QCA-derived DS%, with diagnostic concordance with FFR being 92%, 87%, 76%, and 75%, respectively. Our findings are in line with previous studies showing that purely anatomical parameters have limited diagnostic accuracy⁶. It might be too simplistic to just measure the area or diameter stenosis in a single cross-section, disregarding many other morphologic parameters and the size of downstream perfusion territory which play a crucial role in determining the functional

significance of a coronary stenosis. On the contrary, OFR or QFR integrates the morphological parameters in all the cross-sections along the reconstructed vessel and the estimated perfused flow, resulting in substantial improvement in the diagnosis of functional significance of a coronary stenosis. Remarkably, the present study found very similar diagnostic accuracy as previous studies that used the same algorithms: OFR and OCT-derived MLA by Yu et al.³ where diagnostic concordance with FFR was 90% and 74%, respectively, QFR by Westra et al.⁷ (87%), and 3D QCA-derived DS% by Ding et al (74%)⁸. This demonstrates the robustness of the study findings. The limit of agreement between FFR and OFR is better in the present study compared with the previous study by Yu et al (SD of the difference between OFR and FFR: 0.05 versus 0.07)³. This can possibly be explained by the different lesion characteristics in these two studies. The previous study enrolled patients with more severe stenoses than the present study, with mean FFR of 0.80 compared with 0.82 in the present study. It was shown that numerical deviation of computational FFR with respect to wire-based FFR increased with the lesion severity^{7,9}. Therefore, a narrower limit of agreement between OFR and FFR was found in the present study, when applying the same OFR algorithm.

Comparison between OFR and QFR

Both OFR and QFR are based on fluid dynamics equations that calculate the pressure drop over consecutive segments along the reconstructed vessel. The fundamental difference between these two computational approaches is in the reconstructed lumen geometry and the estimated hyperemic flow. While OCT images provide more accurate

lumen geometry than angiographic images, they are static images providing no information on coronary flow. Therefore, a fixed hyperemic flow velocity of 0.35 m/sec was used for computing OFR. This flow velocity was multiplied by the size of reference coronary artery, i.e., the normal lumen as if there was no stenosis, to obtain patient-specific volumetric flow for the subtended myocardial mass. Seiler et al¹⁰ assessed the relation between coronary artery cross-sectional lumen area and regional myocardial mass and observed a linear correlation in patients without coronary artery disease. This implies that the assumption of a fixed hyperemic flow velocity before developing coronary artery disease is acceptable. Of note, it is crucial to use the reference lumen rather than the actual lumen geometry, since the maximum flow demanded by the subtended myocardial mass will not change as the result of developed epicardial stenosis. Thus, patient-specific maximal flow would have been underestimated if the actual lumen geometry instead of the reference geometry was used to estimate the flow. In the methodology of OFR computation, areas of the side branch ostia were quantified and used to calculate the step-down reference diameter when crossing coronary bifurcations, potentially contributing to an improvement in estimation of maximum flow. On the other hand, coronary angiogram can be used to calculate coronary flow velocity by quantifying the speed of contrast dye in interrogated vessel during wash-in phase. The FAVOR Pilot study showed that the accuracy of QFR computation was improved when using the contrast-flow model compared with fixed-flow model⁴. The subsequent FAVOR II China study that enrolled a much larger study population confirmed the improvement of diagnostic accuracy in QFR by using the contrast-flow

QFR than the fixed-flow QFR. However, the improvement was limited (increase in AUC was 0.02, $p=0.005$)^{5, 11}. Thus, the better accuracy by OFR is not unexpected. It appears that the use of better lumen geometry by OFR outweighs the use of contrast-flow by QFR, resulting in a better diagnostic performance by OFR compared with QFR. This is further confirmed by the result of our subgroup analysis: agreement with FFR was significantly better for OFR than QFR even in patients with prior MI. The finding is clinically relevant since the use of OFR can further improve the accuracy of computational physiological assessment during diagnostic coronary angiography, while OCT also allows assessment of plaque composition and stent expansion/apposition. In addition, OFR can overcome some inherent limitations of angiography-based FFR, i.e. vessel foreshortening and overlap. For those patients with priori high likelihood of PCI, OFR can be included in the present clinical routine for functional evaluation of coronary stenosis without extra instrumentation. For patients presenting with acute coronary syndrome, the use of OCT to assess culprit lesions is recommended¹. In this case, OFR allows more effective assessment of non-culprit lesions that can contribute to the concept of functionally complete revascularization. Moreover, for those patients undergoing subsequent PCI, OFR can be used to improve the functional result of PCI. It was recently reported that significant portion of patients had suboptimal post-procedure FFR¹². Thus, OFR represents a step forward towards precise PCI in compliance with customary reimbursement restrictions. Nevertheless, it should be noted that the current penetration of OCT is still very low in most countries.

Computational FFR in vessels with in-stent restenosis

Disclaimer : As a public service to our readership, this article -- peer reviewed by the Editors of EuroIntervention - has been published immediately upon acceptance as it was received. The content of this article is the sole responsibility of the authors, and not that of the journal

The present study found that the diagnostic accuracy of QFR is reduced in vessels with ISR compared with that in native vessels, despite statistically non-significant (AUC=0.88 versus 0.95, $p=0.102$). For vessels with ISR, QFR correctly classified 82% of the interrogated vessels. This finding is in line with a recent study reporting a 83% diagnostic concordance between QFR and FFR in vessels with ISR¹³. The decrease in diagnostic accuracy in vessels with ISR can possibly be explained by the geometric modeling of QFR, which assumes an elliptical cross-sectional shape in angiographic reconstruction. For vessels with prior implanted stents, the lumen borders are less smoothed and might not be represented by elliptical cross-sections. In addition, stent malapposition and under expansion cannot be identified from angiographic images. Thus, the geometric model based on 3D angiographic reconstruction is less accurate, resulting in impaired accuracy in QFR computation. On the contrary, OCT images allow precise quantification of lumen borders and stent struts, improving the accuracy of geometric model and the subsequent OFR computation. Thus, the diagnostic performance of OFR was excellent in both vessels with ISR and native vessels (AUC=0.96 versus 0.97, $p=0.608$).

Limitations

This study is limited by its retrospective nature. However, all patients undergoing both OCT and FFR were enrolled. Thus, selection bias was avoided. Although following a standard protocol, quite a number of OCT images failed to cover the distal lesion, resulting in 20% of enrolled vessels being excluded for paired OFR and FFR comparison. Nevertheless, latest OCT consoles support longer OCT image pullback that might reduce the chance of not covering the entire lesions. Future studies are needed to assess the feasibility of OFR in a prospective fashion. The present study did not find significant difference in diagnostic accuracy in vessels related with prior MI. However, this result needs to be interpreted with caution. Indeed, correlation between OFR and FFR was numerically lower in vessels related with prior MI. Future dedicated studies are therefore warrant. The incremental value of integrating plaque composition in computational FFR has not been investigated and needs to be understood in future studies.

Conclusions

OFR had an excellent agreement with FFR in consecutive patients with coronary artery disease. OFR was superior to QFR, and much better than conventional morphological parameters in determining physiological significance of coronary stenosis. The diagnostic performance of OFR was not influenced by presence of previously implanted stents.

Impact on daily practice

OFR provides superior diagnostic accuracy in assessing functionally-significant stenosis in addition to other morphological features that can also be assessed simultaneously to better guide and optimize PCI. Moreover, OFR permits the operator to conform to the highest standards currently recommended in PCI, whereas complying with the majority of reimbursement policies in developed countries.

Funding

This work was supported by the Natural Science Foundation of China [grant number 81871460], the National Key Research and Development Program of China [grant number 2016YFC0100500], the Science and Technology Commission of Shanghai Municipality [grant number 18440731700], and by the Program of Shanghai Technology Research Leader.

References

1. Raber L, Mintz GS, Koskinas KC, Johnson TW, Holm NR, Onuma Y, Radu MD, Joner M, Yu B, Jia H. Clinical use of intracoronary imaging. Part 1: guidance and optimization of coronary interventions. An expert consensus document of the European Association of Percutaneous Cardiovascular Interventions. *European Heart Journal* 2018;**39**(35):3281-3300.
2. Xaplanteris P, Fournier S, Pijls NHJ, Fearon WF, Barbato E, Tonino PAL, Engstrom T, Kaab S, Dambrink JH, Rioufol G, Toth GG, Piroth Z, Witt N, Frobert O, Kala P, Linke A, Jagic N, Mates M, Mavromatis K, Samady H, Irimpen A, Oldroyd K, Campo G, Rothenbuhler M, Juni P, De Bruyne B, Investigators F. Five-year outcomes with PCI guided by fractional flow reserve. *N Engl J Med* 2018;**379**(3):250-259.
3. Yu W, Huang J, Jia D, Chen S, Raffel OC, Ding D, Tian F, Kan J, Zhang S, Yan F, Chen Y, Bezerra HG, Wijns W, Tu S. Diagnostic accuracy of intracoronary optical coherence tomography-derived fractional flow reserve for assessment of coronary stenosis severity. *EuroIntervention* 2019;**15**(2):189-197.
4. Tu S, Westra J, Yang J, von Birgelen C, Ferrara A, Pellicano M, Nef H, Tebaldi M, Murasato Y, Lansky A, Barbato E, van der Heijden LC, Reiber JH, Holm NR, Wijns W, Group FPTS. Diagnostic Accuracy of Fast Computational approaches to derive fractional flow reserve from diagnostic coronary angiography: the international multicenter FAVOR Pilot Study. *JACC Cardiovasc Interv* 2016;**9**(19):2024-2035.
5. Xu B, Tu S, Qiao S, Qu X, Chen Y, Yang J, Guo L, Sun Z, Li Z, Tian F, Fang W, Chen J, Li W, Guan C, Holm NR, Wijns W, Hu S. Diagnostic accuracy of angiography-

based quantitative flow ratio measurements for online assessment of coronary stenosis.

J Am Coll Cardiol 2017;**70**(25):3077-3087.

6. Chu M, Dai N, Yang J, Westra J, Tu S. A systematic review of imaging anatomy in predicting functional significance of coronary stenoses determined by fractional flow reserve. Int J Cardiovasc Imaging 2017;**33**(7):975-990.

7. Westra J, Tu S, Campo G, Qiao S, Matsuo H, Qu X, Koltowski L, Chang Y, Liu T, Yang J, Andersen BK, Eftekhari A, Christiansen EH, Escaned J, Wijns W, Xu B, Holm NR. Diagnostic performance of quantitative flow ratio in prospectively enrolled patients: An individual patient-data meta-analysis. Catheter Cardiovasc Interv 2019;**0**(0):693-701.

8. Daixin D, Junqing Y, Westra J, Yundai C, Yunxiao C, Martin H. S-H, Su Z, Evald C, Niels R. H, Bo X, Shengxian T. Accuracy of 3-dimensional and 2-dimensional quantitative coronary angiography for predicting physiological significance of coronary stenosis: A FAVOR II Substudy. Cardiovascular Diagnosis and Therapy 2019;**9**(5):481-491.

9. Cook CM, Petraco R, Shun-Shin MJ, Ahmad Y, Nijjer S, Al-Lamee R, Kikuta Y, Shiono Y, Mayet J, Francis DP, Sen S, Davies JE. Diagnostic accuracy of computed tomography-derived fractional flow reserve : a systematic review. JAMA Cardiol 2017;**2**(7):803-810.

10. Seiler C, Kirkeeide RL, Gould KL. Basic structure-function relations of the epicardial coronary vascular tree. Basis of quantitative coronary arteriography for diffuse coronary artery disease. Circulation 1992;**85**(6):1987-2003.

11. Zhang Y, Zhang S, Westra J, Ding D, Zhao Q, Yang J, Sun Z, Huang J, Pu J, Xu B, Tu S. Automatic coronary blood flow computation: validation in quantitative flow ratio from coronary angiography. *Int J Cardiovasc Imaging* 2019;**35**(4):587-595.
12. Piroth Z, Toth G, Tonino P, Barbato E, Aghlmandi S, Curzen N, Rioufol G, Pijls N, Fearon W, Juni P, Bruyne B. Prognostic value of fractional flow reserve measured immediately after drug-eluting stent implantation. *Circulation: Cardiovascular Interventions* 2017;**10**:e005233.
13. Liontou C, Mejia-Renteria H, Lauri F, Goto S, Lee HJ, Nakayama M, Quiros A, Macaya F, Gonzalo N, Nunez-Gil I, Salinas P, Del Trigo M, Escaned J. Functional assessment of in-stent restenosis with quantitative flow ratio. *EuroIntervention* 2019;Epub ahead of print;DOI: 10.4244/EIJ-D-18-00955.

Figure Legends

Figure 1. Study Flow Chart

FFR=fractional flow reserve; OCT=optical coherence tomography; OFR=optical flow ratio; QFR=quantitative flow ratio.

Figure 2. Histogram distribution of FFR and OFR

Abbreviations as in Figure 1.

Figure 3. Representative Example of Morpho-functional and Morphological Methods in Identifying the Physiological Significance of Coronary Stenosis.

(A) Coronary angiography shows an intermediate LAD lesion. FFR measured by pressure wire at asterisk was 0.68. The computed QFR value is color-coded and superimposed on the 3D angiographic reconstruction. QFR is 0.67 at the most distal position. (B1-B3) correspond to the three positions (white triangles) in panel A. (C) The computed OFR values are colour-coded and superimposed on the 3D OCT reconstruction. OFR is 0.67 at the most distal position. (D) Co-registration between OFR pullback and lumen diameters (short diameter in grey and long diameter in white) for the reconstructed vessel.

LAD=Left anterior descending artery; MLA=minimal lumen area; 3D=three dimensional; other abbreviations as in Figure 1.

Figure 4. Correlation and Agreement for Computational FFR and Wire-based

FFR

(A) Correlation between OFR and FFR. (B) Agreement between OFR and FFR. (C) Correlation between QFR and FFR. (D) Agreement between QFR and FFR.

SD=standard deviation; other abbreviations as in Figure 1.

Figure 5. Comparison of Diagnostic Performance for OFR, QFR, OCT, and 3D

QCA.

OFR showed significantly higher diagnostic accuracy than QFR, OCT-derived MLA, and 3D QCA based DS% in identifying flow-limiting coronary stenosis defined by FFR ≤ 0.80 .

DS%=percent diameter stenosis; QCA=quantitative coronary angiography; other abbreviations as in Figure 1 and Figure 3.

Figure 6. Sensitivity and specificity of Morpho-functional and Morphological

Methods in Identifying the Physiological Significance of Coronary Stenosis

Sensitivity and specificity of OFR, QFR, OCT and 3D QCA: each rectangle in the panel represents the 95% CI of sensitivity and specificity for each method. Wire-based FFR was used as the standard of reference with 100% specificity and sensitivity.

Abbreviations as in Figure 5.

Tables

Table 1. Baseline Demographic Characteristics.

Patients (N=181)	
Patients with FFR measurement in >1 vessel	47 (26.0%)
Age, years	70 [62, 76]
Women	44 (24.3%)
BMI, kg/m ²	24.2±3.6
Diabetes Mellitus	77 (42.5%)
Hypertension	149 (82.3%)
Hyperlipidemia	133 (73.5%)
Current Smoker	36 (19.9%)
Family History of CAD	40 (22.1%)
Previous PCI	118 (65.2%)
Previous CABG	3 (1.7%)
Previous MI	81 (44.8%)
Clinical Presentation	
Silent Ischemia	88 (48.6%)
Stable Angina	49 (27.1%)
Unstable Angina	25 (13.8%)
NSTEMI	6 (3.3%)
Others	13 (7.2%)

Disclaimer : As a public service to our readership, this article -- peer reviewed by the Editors of EuroIntervention - has been published immediately upon acceptance as it was received. The content of this article is the sole responsibility of the authors, and not that of the journal

Data are presented as mean±SD, n (%) or median (interquartile range).

BMI=body mass index; CABG=coronary artery bypass surgery; CAD=coronary artery disease; FFR=fractional flow reserve; MI=myocardial infarction; NSTEMI: non-ST segment elevation myocardial infarction; PCI=percutaneous coronary intervention.

Copyright EuroIntervention

Table 2. Baseline Vessel Characteristics

Vessels (N=212)	
Interrogated Vessel	
Left Anterior Descending	128 (60.4%)
Diagonal	1 (0.5%)
Left Circumflex	36 (17.0%)
Obtuse Marginal	1 (0.5%)
Right Coronary Artery	46 (21.7%)
Lesion Location	
Proximal	75 (35.4%)
Middle	101 (47.6%)
Distal	36 (17.0%)
Bifurcation Lesions	97 (45.8%)
Tandem Lesions	47 (22.2%)
Diffuse Disease	80 (37.7%)
Analyzed OCT pullback Length, mm	56.1 [49.8, 66.3]
Lesion Length*, mm	19.5 [12.6, 30.0]
Percent Diameter Stenosis*, %	49.4±11.7
Reference Vessel Diameter*, mm	2.75 [2.40, 3.10]
Minimum Lumen Area, mm ²	1.92 [1.29, 2.48]
FFR Data	

Disclaimer : As a public service to our readership, this article -- peer reviewed by the Editors of EuroIntervention - has been published immediately upon acceptance as it was received. The content of this article is the sole responsibility of the authors, and not that of the journal

FFR	0.82±0.10
FFR≤0.80	85 (40.1%)
0.75≤FFR≤0.85	77 (36.3%)

Data are presented as mean±SD or n (%). *Assessed by 3D QCA.

OCT=optical coherence tomography; 3D QCA = three dimensional quantitative coronary angiography; other abbreviations as in Table 1.

Copyright EuroIntervention

Table 3. Diagnostic Performance of OFR, QFR, OCT-derived MLA and 3D QCA-derived DS% in predicting FFR \leq 0.80

	OFR \leq 0.80	OCT-derived MLA \leq 1.88	QFR \leq 0.80	3D QCA- derived DS% $>$ 50.7%
Accuracy	92 (88-95)	76 (70-82)	87 (83-92)	75 (69-80)
Sensitivity	86 (77-93)	79 (69-87)	88 (79-94)	74 (64-83)
Specificity	95 (90-98)	74 (66-81)	87 (80-93)	75 (66-82)
PPV	92 (84-97)	67 (57-76)	82 (73-90)	66 (56-76)
NPV	91 (85-95)	84 (76-90)	92 (85-96)	81 (73-88)
+LR	18.2 (8.3-39.9)	3.0 (2.2-4.2)	7.0 (4.4-11.1)	2.9 (2.1-4.1)
-LR	0.2 (0.1-0.3)	0.3 (0.2-0.4)	0.1 (0.1-0.2)	0.4 (0.2-0.5)
AUC	0.97 (0.93- 0.99)	0.82 (0.76- 0.87)	0.92 (0.87- 0.95)	0.80 (0.74- 0.85)

Results are percentage (95% confidence interval) except area under the curve (AUC) and likelihood ratios.

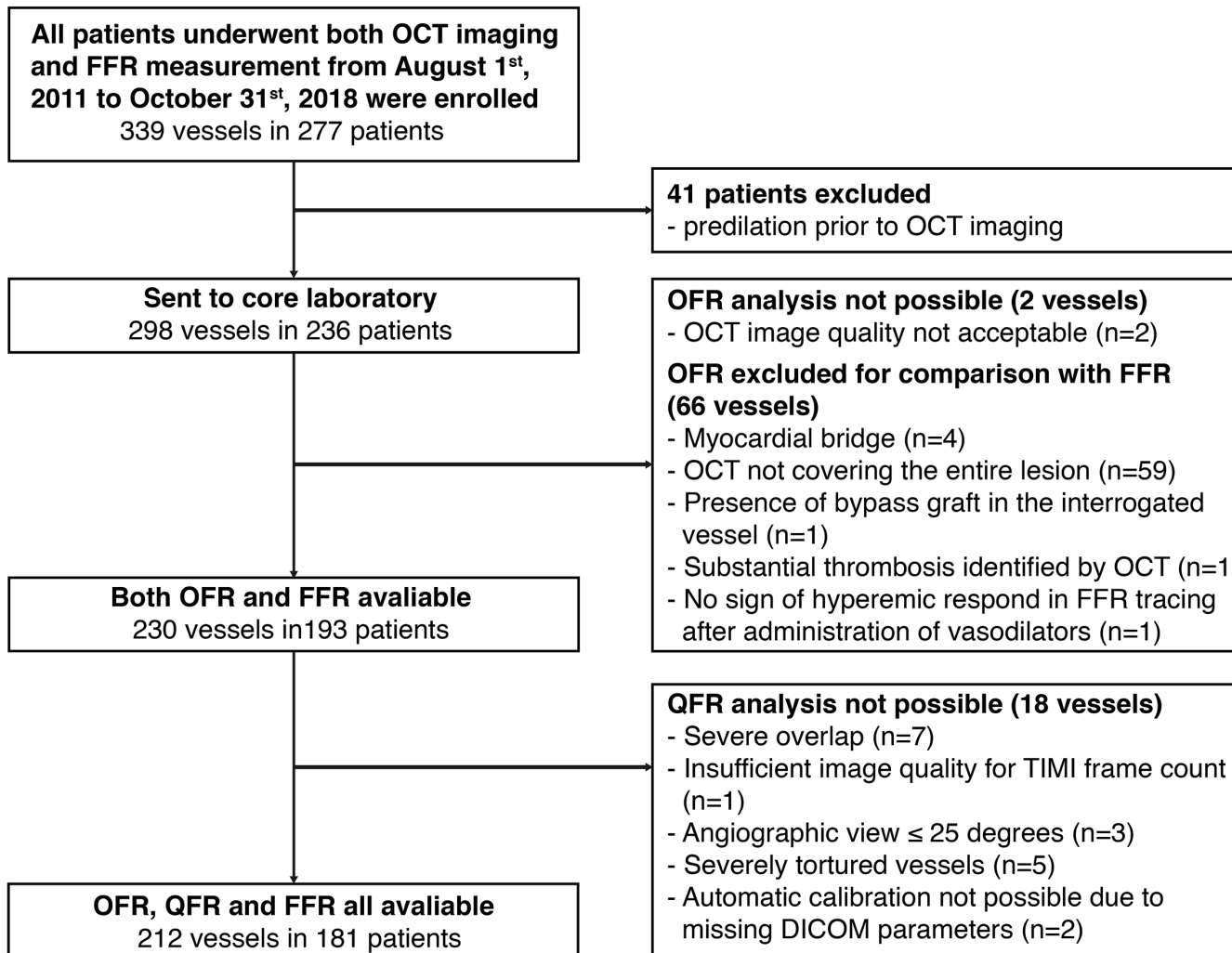
DS=diameter stenosis; MLA=minimum lumen area; NPV=negative predictive value;

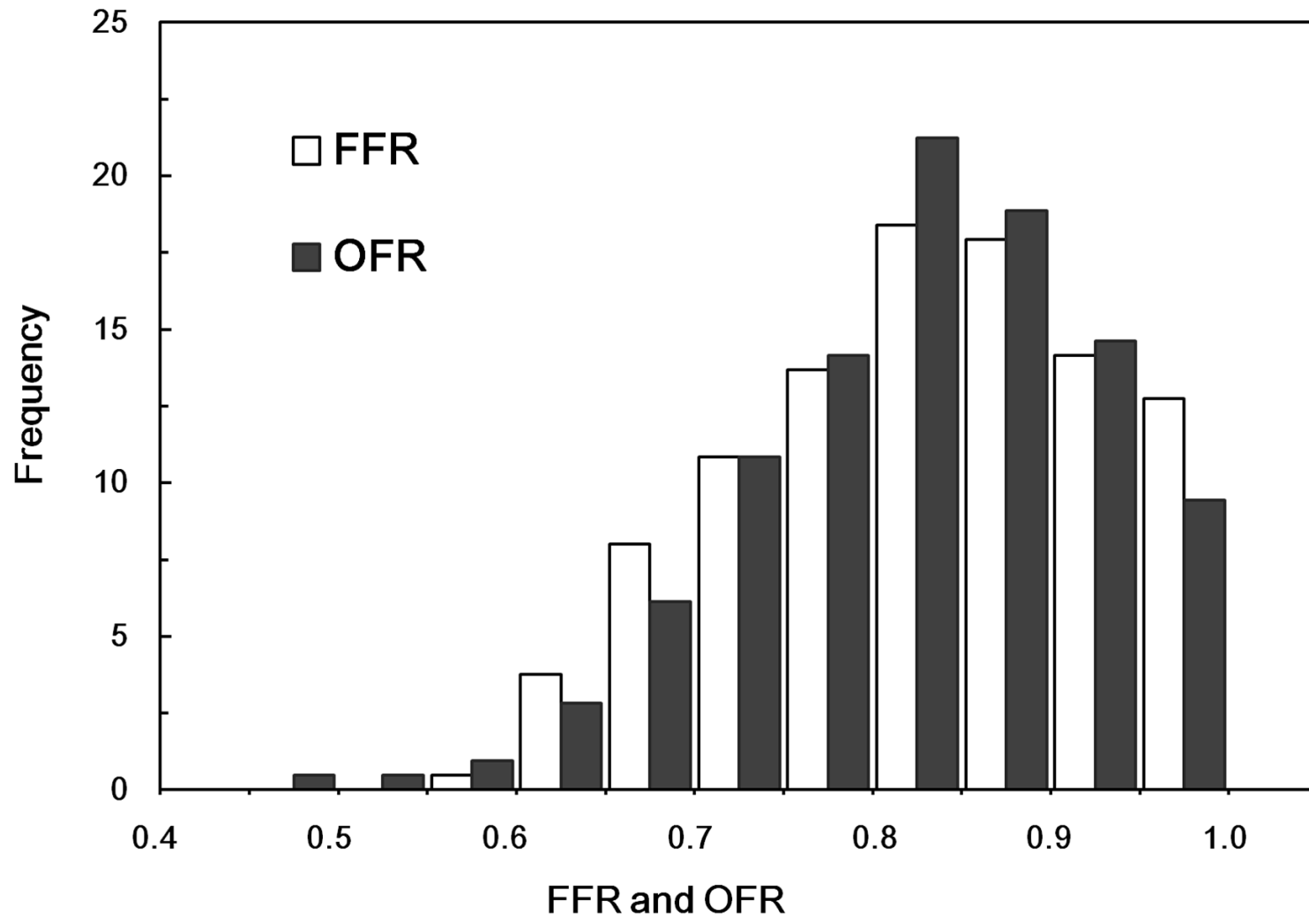
OFR=optical flow ratio; PPV=positive predictive value; QFR=quantitative flow

ration; +LR=positive likelihood ratio; -LR=negative likelihood ratio; other

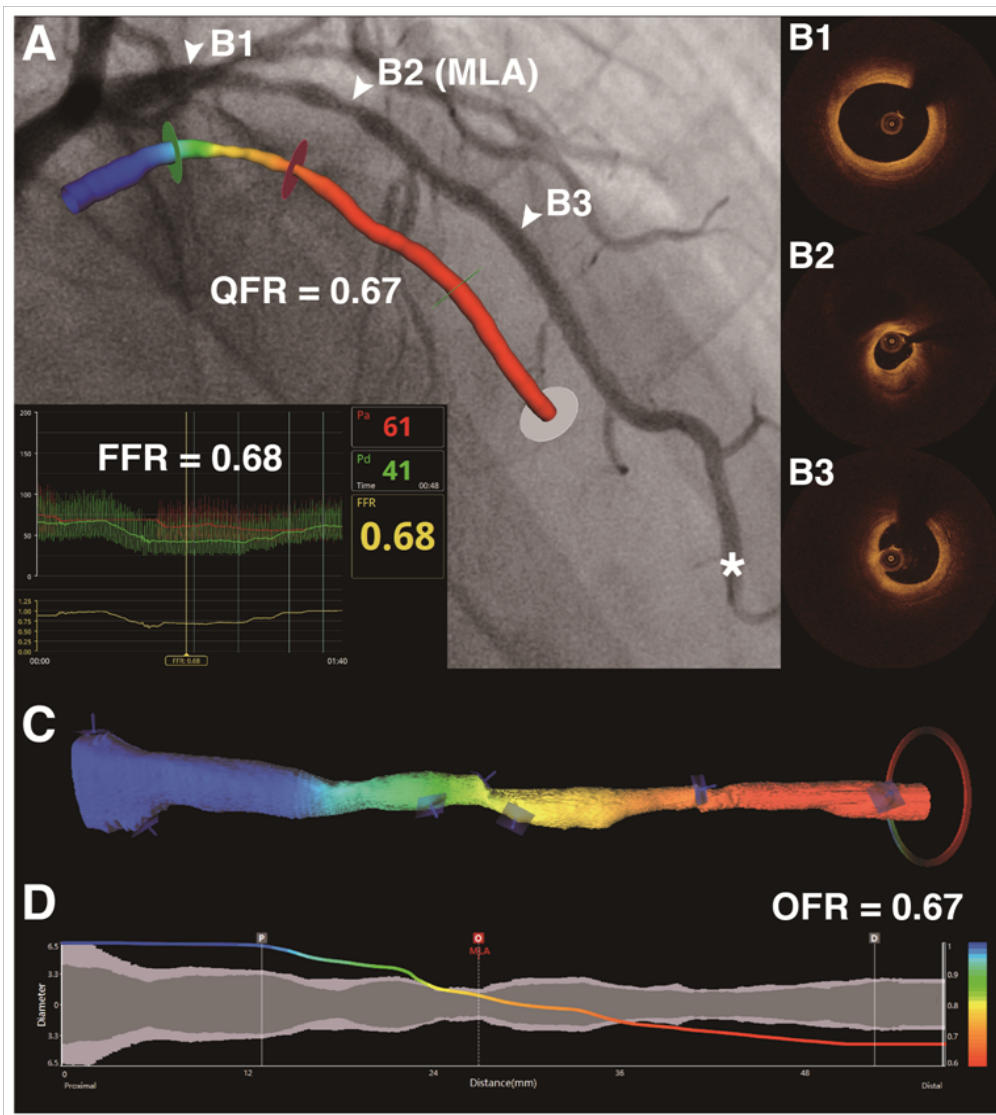
abbreviations as in Table 1 and 2.

Disclaimer : As a public service to our readership, this article -- peer reviewed by the Editors of EuroIntervention - has been published immediately upon acceptance as it was received. The content of this article is the sole responsibility of the authors, and not that of the journal



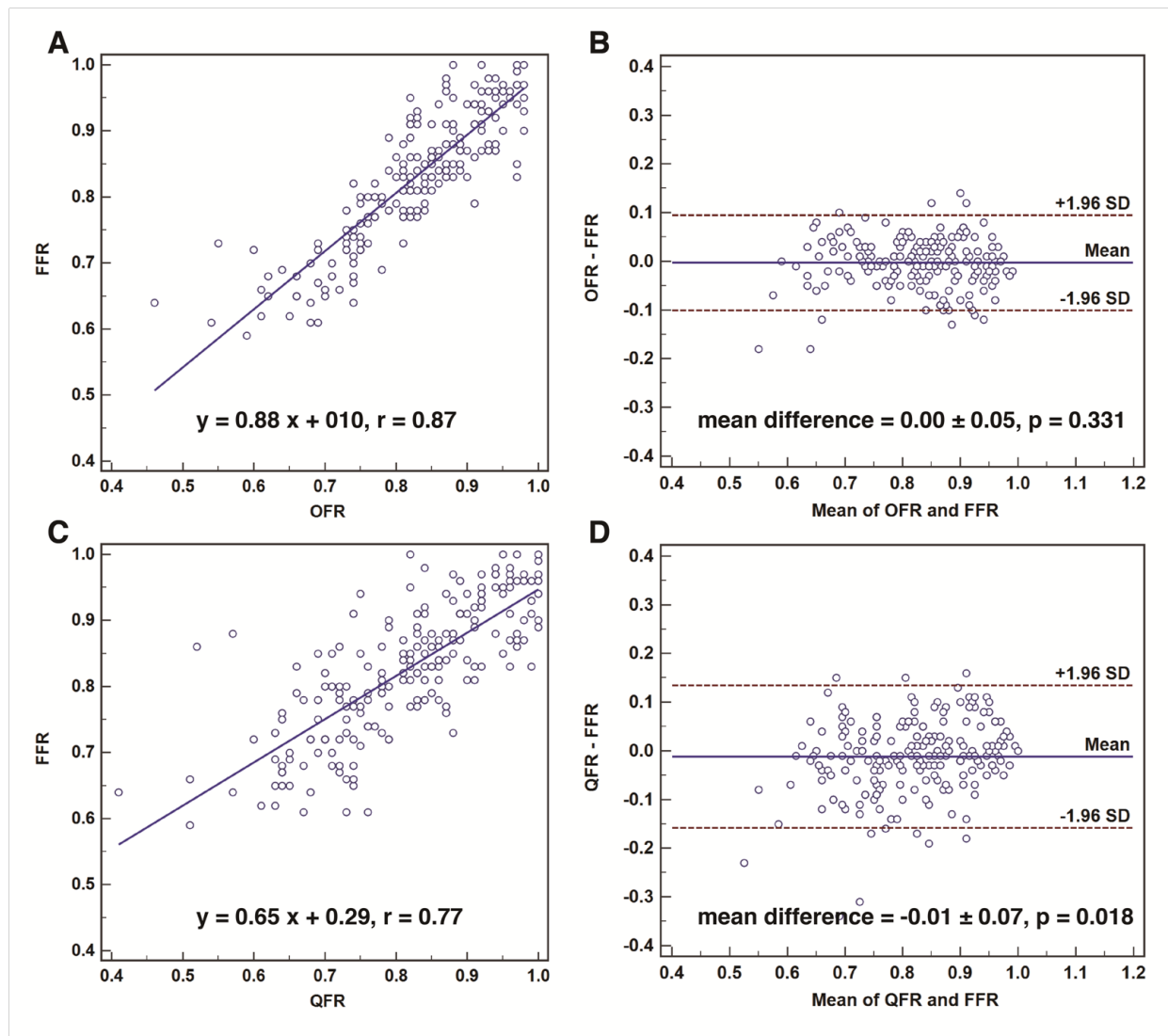


Disclaimer : As a public service to our readership, this article -- peer reviewed by the Editors of EuroIntervention - has been published immediately upon acceptance as it was received. The content of this article is the sole responsibility of the authors, and not that of the journal

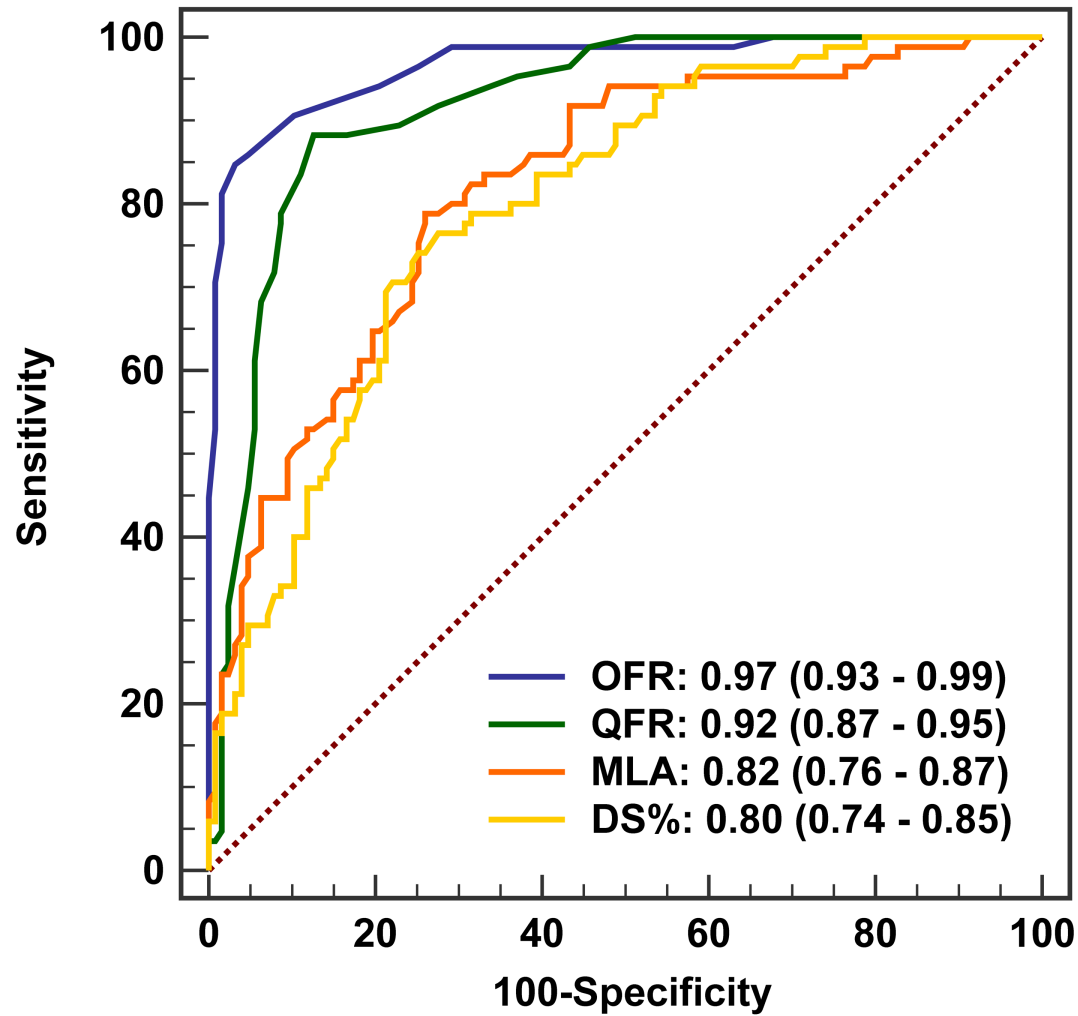


intervention

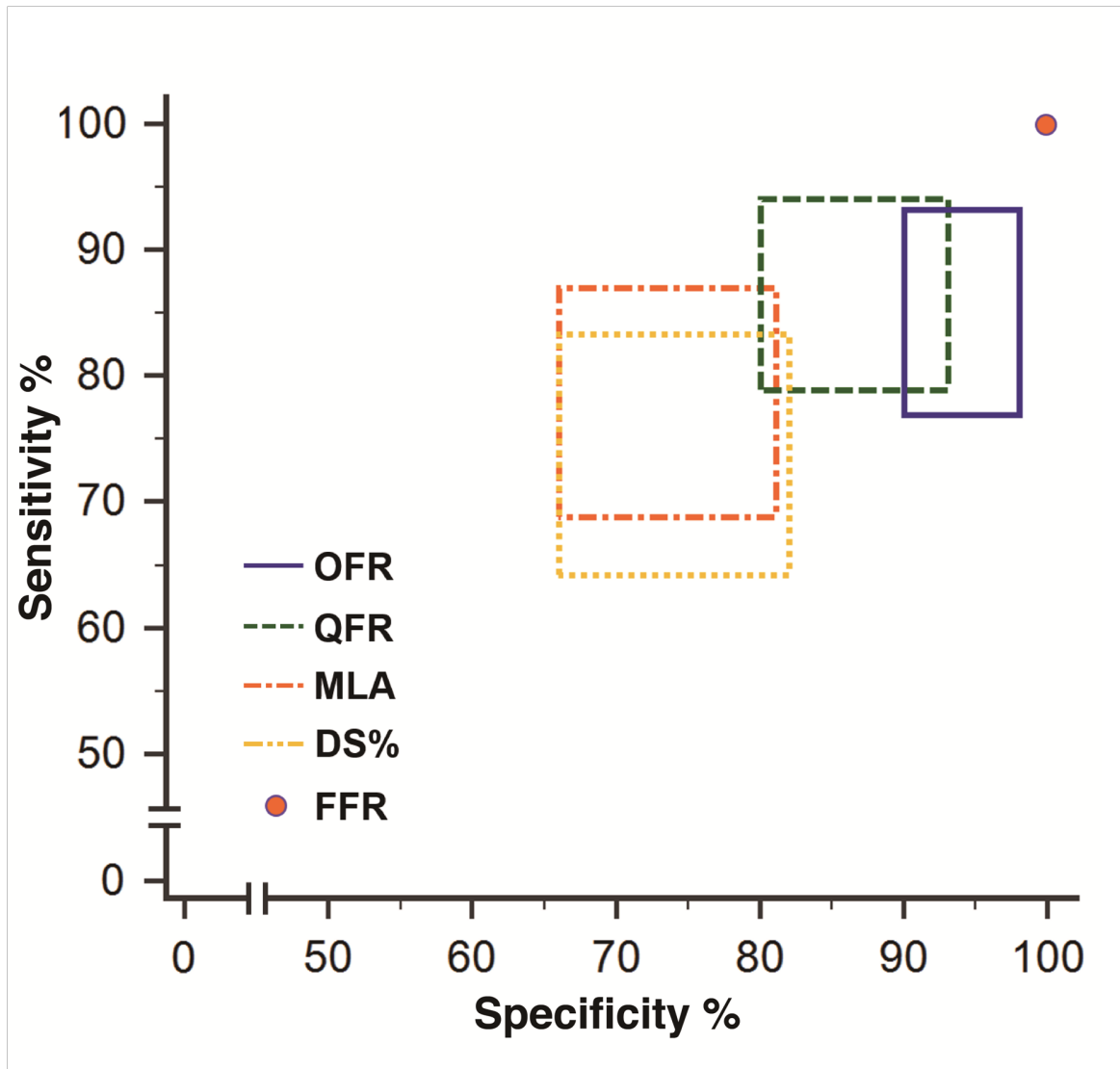
Disclaimer : As a public service to our readership, this article -- peer reviewed by the Editors of EuroIntervention - has been published immediately upon acceptance as it was received. The content of this article is the sole responsibility of the authors, and not that of the journal



Disclaimer : As a public service to our readership, this article -- peer reviewed by the Editors of EuroIntervention - has been published immediately upon acceptance as it was received. The content of this article is the sole responsibility of the authors, and not that of the journal



Disclaimer : As a public service to our readership, this article -- peer reviewed by the Editors of EuroIntervention - has been published immediately upon acceptance as it was received. The content of this article is the sole responsibility of the authors, and not that of the journal



Disclaimer : As a public service to our readership, this article -- peer reviewed by the Editors of EuroIntervention - has been published immediately upon acceptance as it was received. The content of this article is the sole responsibility of the authors, and not that of the journal

Supplementary Data

Supplementary data for coronary angiography, FFR and OCT	3
Supplementary data for the co-registration of FFR, OFR and QFR	5
Supplementary data for combining OFR from two OCT pullbacks	6
Supplementary data for the diagnostic accuracy of OFR in the measurement grayzone	7
Supplementary Tables	8
Supplementary Figures	9

Supplementary data for coronary angiography, FFR and OCT

Invasive coronary angiography

Invasive coronary angiography was performed with 5- or 6- French catheter using the transfemoral or the transradial approach. Contrast media (Omnipaque 350 Injection, Daiichi Sankyo Co., Ltd., Tokyo, Japan) was injected into the coronary artery at a rate of 2-4 mL/sec for approximately 2-3 sec using an injector pump (Mark V, Medrad, PA, USA). Coronary angiograms were recorded using monoplane or biplane X-ray angiogram (Allura Xper FD 10, Philips Healthcare, Best, The Netherlands) at 15 frames/sec.

Fractional flow reserve

FFR measurement was performed at operator's discretion using a 0.014-inch pressure wire (St Jude Medical, Uppsala, Sweden) or PrimeWire Prestige (Philips Volcano, San Diego, California, USA). The pressure wire was calibrated at the tip of the guiding catheter and subsequently positioned distal to the coronary stenosis. The position of the sensor or the pressure wire was recorded on angiograms. A continuous intravenous infusion of 150 µg/kg/min adenosine 5'-triphosphate was used to induce maximal hyperemia. The pressure wire was pulled back manually during steady-state maximal hyperemia. At the end of the pullback, pressures at the tip of the guiding catheter were examined to exclude pressure drift. The drift was deemed unacceptable if exceeding 3 mmHg. In such cases, the FFR measurement was repeated.

Disclaimer : As a public service to our readership, this article -- peer reviewed by the Editors of EuroIntervention - has been published immediately upon acceptance as it was received. The content of this article is the sole responsibility of the authors, and not that of the journal

Analysis of all FFR pressure tracings were performed at the Wakayama Medical University Hospital, using the minimal and stable position during hyperemia for FFR reading.

OCT imaging

OCT imaging was performed at operator's discretion using frequency-domain OCT systems (ILUMIEN™ or OPTIS™; Abbott, St. Paul, MN, USA), with the Dragonfly or Dragonfly DUO catheter. The fiber probe was pulled back within the stationary imaging sheath. Cross-sectional images were generated at a rotational speed of 100 or 180 frames/sec.

Supplementary data for the co-registration of FFR, OFR and QFR

At Wakayama Medical University Hospital, the pressure wire and the OCT imaging catheter were filmed when advanced distally to the stenosis. At the imaging core laboratory, the OCT imaging segment was first co-registered with the angiographic images by correlating the OCT side branches with the angiographic side branches. Subsequently, the vessel segment corresponding to the OCT image pullback was marked in angiographic images to examine whether there was still proximal or distal stenosis not covered. If so, the vessel will be excluded for the analysis. It is true that the manual co-registration might not be 100% accurate. However, the impact was relatively small as long as the distal position lands on a normal segment, since including longer normal segment in the computational analysis will not have much pressure drop. Thus, the impact on the correlation between QFR and OFR is negligible.

Supplementary data for combining OFR from two OCT pullbacks

For interrogated vessels with two OCT pullbacks to cover the entire lesion, the OFR value would be computed for each pullback and combined to generate the final OFR value at the most distal position, using the following formula:

$$OFR_{combined} = OFR_{pullback1} + OFR_{pullback2}$$

As is shown in Supplementary Figure 1, when analyzing overlapping OCT pullbacks, the overlapping part would be excluded from the region of interest for the second pullback, ensuring that the pressure drop of the overlapping part would only be counted once to generate the final OFR value.

Supplementary data for the diagnostic accuracy of OFR in the measurement grayzone

A total of 77 (36.3%) vessels had FFR value falling in the measurement gray zone between 0.75 and 0.85. The numerical difference between OFR and FFR were comparable inside and outside the measurement gray zone (0.01 ± 0.04 versus -0.01 ± 0.05 , $p=0.004$). However, the diagnostic concordance between OFR and FFR was significantly lower inside the measurement grayzone (81% [95% CI: 71%-90%] versus 98% [95% CI: 95%-100%], $p<0.001$). This is expected since any binary diagnostic metric will have lower diagnostic accuracy when approaching the cutoff value. Previous study also reported that the diagnostic accuracy of FFR itself would fall to around 80% in the zone between 0.77 and 0.83 (DOI 10.1016/j.jcin.2012.10.014).

Supplementary Tables

Supplementary Table 1. Comparison of intraclass correlation coefficients in different vessels

	OFR and FFR	QFR and FFR	p value
LAD (n=129)	0.89 (0.84-0.92)	0.69 (0.59-0.77)	p<0.001
Non-LAD (n=83)	0.78 (0.66-0.86)	0.76 (0.64-0.85)	p=0.751

Copyright EuroIntervention

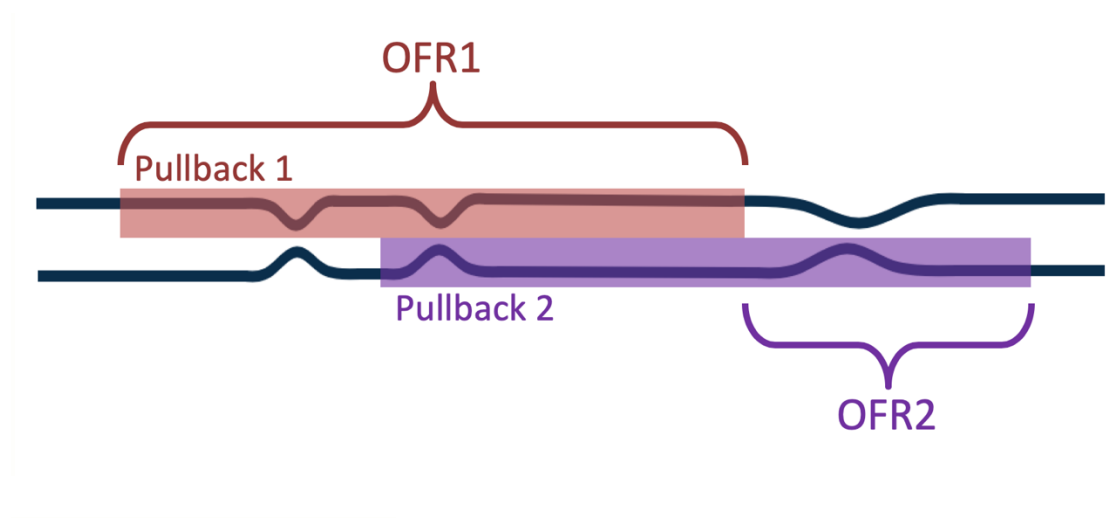
Supplementary Figures

Supplementary Figure 1. Combine OFR from two OCT pullbacks

Supplementary Figure 2. Classification agreement between computational FFR and wire-based FFR: V-plot of the classification agreement between OFR and FFR (A), and QFR and FFR (B)

Copyright EuroIntervention

Supplementary Figure 1:



Copyright EuroIntervention

Supplementary Figure 2:

